LOFTID Surface Heating Reconstruction

H. S. Alpert[1] and S. Tobin[2], [1]NASA Ames, Moffett Field, CA (hannah.s.alpert@nasa.gov), [2]NASA Langley, Hampton, VA

Brief Author Biography: Hannah Alpert received her PhD in Aeronautics and Astronautics from Stanford University. She is currently working as an Aerospace Systems Engineer at NASA Ames Research Center in the Entry Systems and Vehicle Development Branch.

Introduction: On November 10, 2022, the Low-Earth Orbit Flight Test of an Inflatable Decelerator (LOFTID) reentry vehicle launched to low-Earth orbit aboard a United Launch Alliance Atlas V rocket out of Vandenberg Air Force Base. The aeroshell, the largest Hypersonic Inflatable Aerodynamic Decelerator (HIAD) ever flown, was inflated to its full 6-meter diameter before successful re-entry into the atmosphere. The aeroshell was heavily instrumented in order to understand its behavior during entry. There were 82 thermocouples (TCs) distributed across the aeroshell, with 22 integrated into the flexible thermal protection system (FTPS) on the rigid nose, 36 in the FTPS on the deployable structure, and 24 on the inflatable structure. TCs were placed at different depths throughout the FTPS. Those nearest to the surface were located just beneath the two SiC outer fabric layers. The near-surface TCs on the rigid nose were Type R with flame spray alumina insulation, while those on the flank were Type N with mica/ceramic insulation. Additionally, a radiometer was placed at the center of the nose surrounded by four total heat flux gauges in a cruciform configuration at a radius of 0.41 m [1]. The nose instrumentation is shown in Fig. 1 and a cross-section of the aeroshell with all TC locations is shown in Fig. 2. The objective of this work was to use the temperatures measured by the TCs during flight to estimate the surface heat rate across the aeroshell throughout the period of re-entry by inverse analysis methodology. The results were used to evaluate the fidelity of measurements from the total heat flux gauges on the nose, determine the surface heat flux at aeroshell locations where gauges were not present, and compare to pre-flight CFD-based heating predictions. Inversely estimated surface heat flux continues to be used to correlate FTPS thermal models to reconstruct in-flight thermal response.

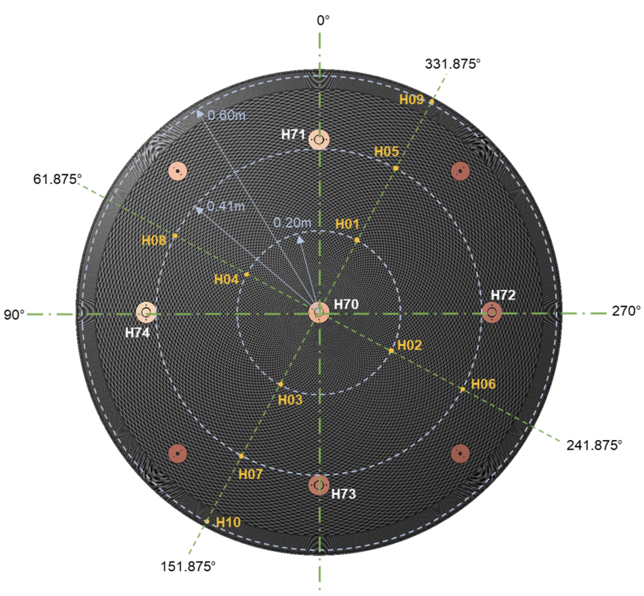

Figure 1: **Instrumentation on the nose.**

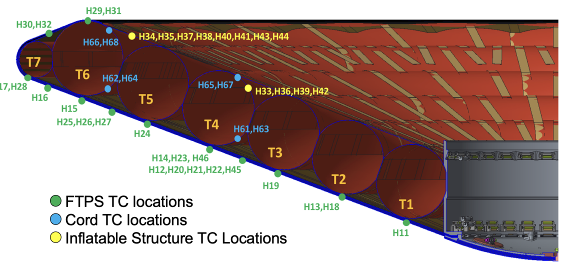

Figure 2: **Cross section of the aeroshell showing TC locations.**

Inverse Surface Heating Methodology: A detailed thermal model was created in COMSOL Multiphysics® prior to flight to generate heating predictions through the depth of the FTPS [2]. To perform the surface heating reconstruction, COMSOL's Optimization Module [3] was incorporated into the existing thermal model. The inputs to the optimization were 1) the near-surface TC data from flight, as the target temperature for the model to match, 2) an initial guess of the surface heat flux (e.g., the pre-flight prediction), and 3) optimization parameters, including the choice of control function, optimization solver, and solver parameters. The objective function for the optimization was the difference of squares of the model temperature at the depth of the TC and the TC flight data, throughout the heating pulse. The control function selected for this study was a Bernstein polynomial of order 20. The coefficients of this polynomial were optimized such that when the function was multiplied by the initial guess of the heat flux, the result was the optimized heat flux. For the solver, the gradient-free Bound Optimization by Quadratic Approximation (BOBYQA) method was employed. The same optimization method was employed on the convective heat transfer coefficient (C_H) instead of the initial heat flux – the Bernstein polynomial was optimized such that when multiplied by C_H, the in-depth temperature matched the flight temperature, and the resulting heat flux could be measured in the model. The two methods gave similar results.

Results and Discussion: Models were run to estimate surface heating at the following TC locations: two of the TCs closest to the center (LTH01 and LTH02), one TC at the same radial as the total heat flux gauges (LTH08), one TC on the second torus from the nose (LTH18), and one TC on the flank between the third and fourth tori (LTH21). As an example, the results for LTH18 are shown in Fig. 3, where the dashed blue line in Fig. 3a is the pre-flight predicted heat flux and the solid blue line in Fig. 3b is the temperature predicted at the TC location due to the predicted heat flux. The solid green line is the flight data from LTH18. The dashed orange line in Fig. 3a is the reconstructed surface heat flux that was calculated after running the optimization. Finally, the solid orange line in Fig. 3b is the temperature at the LTH18 location due to the optimized surface heat flux being applied. The solid orange and green lines align quite well with one another, showing that the optimized heat flux produces a temperature profile very similar to the flight data. The other four TCs showed similar results to the LTH18 case.

The heat flux at the LTH08 location was reconstructed to enable a comparison between the reconstructed heat flux and the heat flux measured by the total heat flux gauges. In addition to the case with nominal material properties, cases were also run with stacked 1σ departures from nominal SiC

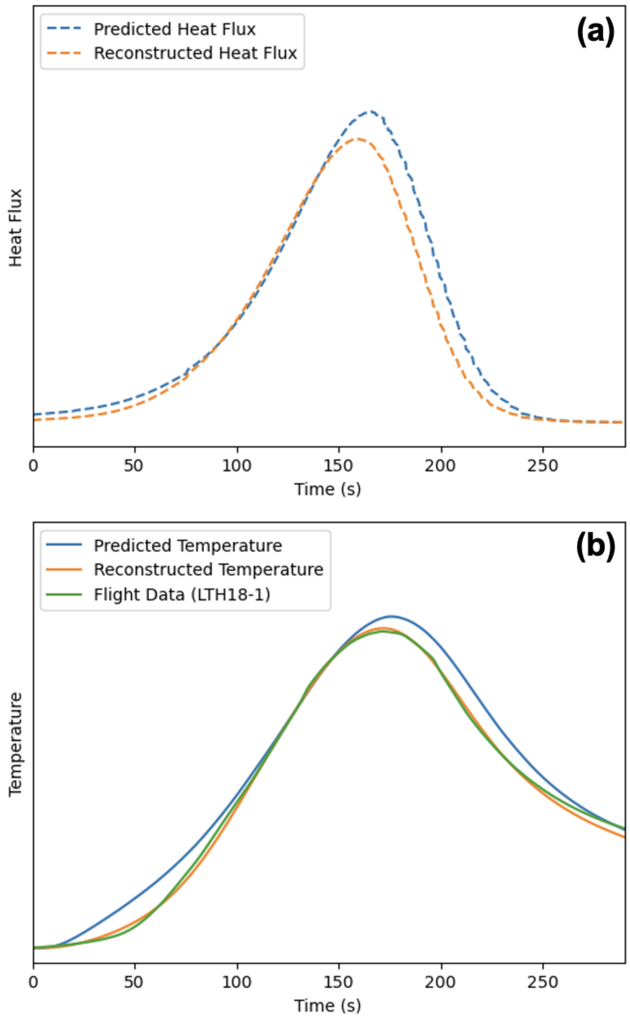

Figure 3: **Plots for LTH18 of (a) predicted heat flux (blue dashed line) vs. reconstructed heat flux (orange dashed line) and (b) predicted temperature at LTH18 location (blue solid line), temperature measured by LTH18 during flight (green solid line), and model temperature when reconstructed heat flux is applied (orange solid line).**

material properties and maximum TC measurement errors to produce low and high uncertainty bounds.The nominal reconstructed heat flux at the LTH08 location was higher than that measured by the heat flux gauges; thus, this analysis was conducted to assess whether the flight data was within the uncertainty bounds of the reconstructed heat flux with these uncertainties included. In order to make a comparison between the reconstructed heat flux and heat flux gauge measurements, a correction had to be made to account for the fact that the FTPS was at a much higher temperature than the heat flux gauge, which was surrounded by a copper heat sink. After including the correction, the cold wall heat flux on the gauge was estimated to be about 6% higher than the hot wall heat flux on the FTPS. A comparison between the heat flux gauge data and the reconstructed cold wall heat flux is shown in Fig. 4.

The fact that the heat flux gauge data departs from the nominal reconstructed heat flux profile after about 80 seconds, and is outside the uncertainty bounds of the reconstructed heat flux near the peak suggests that the heat flux gauge measurements may not accurately represent the heat flux on the FTPS. One possible reason for this is the presence of a ring of RTV sealant between the heat sink and the FTPS, products from which may have interfered with the measurement of surface heat flux. A second hypothesis is that the flat large copper sensor housing and heat sink sat slightly recessed compared to the FTPS, which may have affected the heat flux detected at the gauge location.

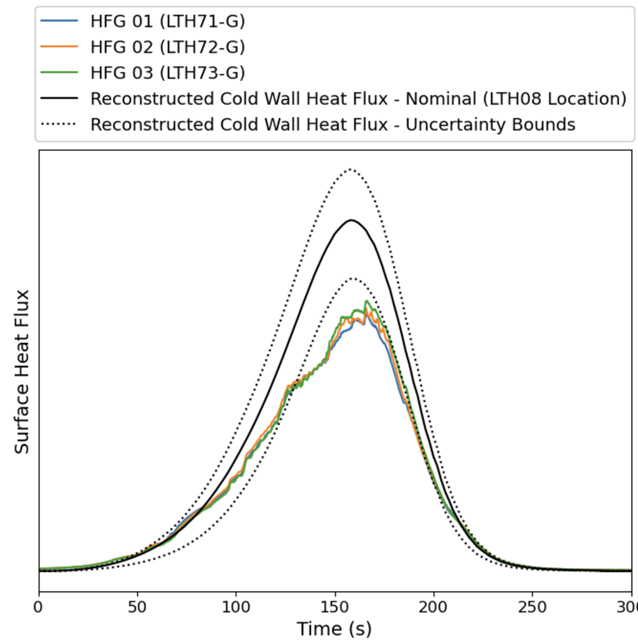

Figure 4: **Comparison between heat flux gauge measurements and reconstructed heat flux at LTH08 location with uncertainty bounds.**

Further work includes conducting a similar inverse heating reconstruction process for more flank and shoulder TC locations. The results will contribute to the FTPS/aeroshell thermal response model correlation, which will aid in the improvement of design tools for future HIAD missions.

References:

[1] Swanson, G., et al. (2024) *AIAA SciTech*.

[2] Tobin, S., et al. (2024) *AIAA SciTech*.

[3] *COMSOL Optimization Module User's Guide*.